

RESEARCH ARTICLE

Correlation of histopathologic characteristics to protein expression and function in malignant melanoma

Charlotte Welinder^{1,2}, Krzysztof Pawłowski^{3,4}, A. Marcell Szasz^{1,2,5}, Maria Yakovleva², Yutaka Sugihara¹, Johan Malm^{2,4}, Göran Jönsson¹, Christian Ingvar⁶, Lotta Lundgren^{1,7}, Bo Baldetorp¹, Håkan Olsson^{1,7,8}, Melinda Rezeli⁹, Thomas Laurell^{2,9}, Elisabet Wieslander¹, György Marko-Varga^{2,9,10*}

1 Division of Oncology and Pathology, Dept. of Clinical Sciences Lund, Lund University, Lund, Sweden, **2** Centre of Excellence in Biological and Medical Mass Spectrometry “CEBMMS”, Biomedical Centre D13, Lund University, Lund, Sweden, **3** Faculty of Agriculture and Biology, Dept. of Experimental Design and Bioinformatics, Warsaw University of Life Sciences, Warszawa, Poland, **4** Dept. of Translational Medicine, Lund University, Malmö, Sweden, **5** 2nd Dept. of Pathology, Semmelweis University, Budapest, Hungary, **6** Dept. of Surgery, Dept. of Clinical Sciences Lund, Lund University, Skåne University Hospital, Lund, Sweden, **7** Dept. of Oncology, Skåne University Hospital, Lund, Sweden, **8** Cancer Epidemiology, Dept. of Clinical Sciences, Lund University, Lund, Sweden, **9** Clinical Protein Science & Imaging, Biomedical Centre, Dept. of Biomedical Engineering, Lund University, BMC D13, Lund, Sweden, **10** First Dept. of Surgery, Tokyo Medical University, Tokyo, Japan

* Gyorgy.Marko-Varga@bme.lth.se



OPEN ACCESS

Citation: Welinder C, Pawłowski K, Szasz AM, Yakovleva M, Sugihara Y, Malm J, et al. (2017) Correlation of histopathologic characteristics to protein expression and function in malignant melanoma. PLoS ONE 12(4): e0176167. <https://doi.org/10.1371/journal.pone.0176167>

Editor: Michal Zmijewski, Medical University of Gdańsk, POLAND

Received: October 31, 2016

Accepted: April 6, 2017

Published: April 26, 2017

Copyright: © 2017 Welinder et al. This is an open access article distributed under the terms of the [Creative Commons Attribution License](https://creativecommons.org/licenses/by/4.0/), which permits unrestricted use, distribution, and reproduction in any medium, provided the original author and source are credited.

Data Availability Statement: Proteomics data were used, as deposited in the PRIDE database, under the dataset identifier PXD001725.

Funding: This study was supported by grants from Mrs. Berta Kamprad Foundation, Vinnova, Inga-Britt and Arne Lundbergs Foundation, The Crafoord Foundation, and European Research Council Advanced Grant. The funders had no role in study design, data collection and analysis, decision to publish, or preparation of the manuscript.

Abstract

Background

Metastatic melanoma is still one of the most prevalent skin cancers, which upon progression has neither a prognostic marker nor a specific and lasting treatment. Proteomic analysis is a versatile approach with high throughput data and results that can be used for characterizing tissue samples. However, such analysis is hampered by the complexity of the disease, heterogeneity of patients, tumors, and samples themselves. With the long term aim of quest for better diagnostics biomarkers, as well as predictive and prognostic markers, we focused on relating high resolution proteomics data to careful histopathological evaluation of the tumor samples and patient survival information.

Patients and methods

Regional lymph node metastases obtained from ten patients with metastatic melanoma (stage III) were analyzed by histopathology and proteomics using mass spectrometry. Out of the ten patients, six had clinical follow-up data. The protein deep mining mass spectrometry data was related to the histopathology tumor tissue sections adjacent to the area used for deep-mining. Clinical follow-up data provided information on disease progression which could be linked to protein expression aiming to identify tissue-based specific protein markers for metastatic melanoma and prognostic factors for prediction of progression of stage III disease.

Competing interests: The authors have declared that no competing interests exist.

Results

In this feasibility study, several proteins were identified that positively correlated to tumor tissue content including IF6, ARF4, MUC18, UBC12, CSPG4, PCNA, PMEL and MAGD2. The study also identified MYC, HNF4A and TGFB1 as top upstream regulators correlating to tumor tissue content. Other proteins were inversely correlated to tumor tissue content, the most significant being; TENX, EHD2, ZA2G, AOC3, FETUA and THRB. A number of proteins were significantly related to clinical outcome, among these, HEXB, PKM and GPNMB stood out, as hallmarks of processes involved in progression from stage III to stage IV disease and poor survival.

Conclusion

In this feasibility study, promising results show the feasibility of relating proteomics to histopathology and clinical outcome, and insight thus can be gained into the molecular processes driving the disease. The combined analysis of histological features including the sample cellular composition with protein expression of each metastasis enabled the identification of novel, differentially expressed proteins. Further studies are necessary to determine whether these putative biomarkers can be utilized in diagnostics and prognostic prediction of metastatic melanoma.

Introduction

Cutaneous metastatic melanoma (MM) is the sixth most common cancer worldwide with an increasing incidence especially in the Northern European countries and Australia [1, 2]. In Sweden it is the fifth most prevalent malignant neoplasm both in men (following prostate, colon, non-melanocytic skin and urinary tract tumors) and women (following breast, colon, non-melanocytic skin and uterine neoplasms) with an annual incidence of 5% [3, 4].

Malignant melanoma possessing a wide variety of cytomorphologic features can be considered as a challenge from a diagnostic perspective, and is well-known for its metastatic spread, most common to the lungs, liver, brain, bone and skin but sometimes to any, and often unusual location in the body. Melanoma tumors commonly possess a broad toolkit to escape from the body surveillance system [5] thus facilitating further metastatic spread. Examples of such mechanisms are replicative immortality, genome instability and mutation, resistance to cell death, deregulated cellular energetics, sustaining proliferative signaling, evasion of growth suppressors, activation of invasion and metastasis, tumor promoting inflammation and means to avoid immune destruction [6].

Screening and early detection improve survival from MM and a better outcome can be expected once surgical removal of early primary lesion was performed, still about 15–25% of the sentinel lymph nodes contain metastatic melanoma cells [7]. Progression from the lymph nodes may occur with time, and metastatic melanoma has been inherently difficult to treat with a low survival rate (< 15% at 5 years) [8]. A phase 3 clinical trial (Multicenter Selective Lymphadenectomy Trial II, or MSLT-II) is designed and conducted to answer the question whether sentinel lymph node biopsy should routinely be followed by removal of the remaining regional lymph nodes (complete lymph node dissection) if the sentinel lymph node is positive for melanoma, or it should be followed-up by ultrasound [9].

Factors determining prognosis routinely rely on clinicopathological characteristics of the patient and primary tumor [10–13], which have been supplemented with DNA sequencing

studies in the past years [14–20]. Most melanomas harbor alterations in the BRAF, NF1, RAS, MDM2 (KIT) genes, which result in activation of the MAPK and RAS pathways conferring survival advantage by reprogramming crucial cell cycle and apoptotic cellular functions [21]. Clinical and pathological properties partly reflect the identified (BRAF, RAS, NF1, triple wild type) genomic subtypes of melanoma, but from both clinical and genetic perspective the groups still are heterogeneous [21].

Newly developed drugs allowing targeted therapy such as kinase inhibitors or drugs modulating the immune response currently provide more promise to the patients [22–27]. However, some of these newer treatments have also been subjected to the development of resistance [28]. Recently, the Food and Drug Administration (FDA) approved nivolumab (Opdivo), a PD-1 immune checkpoint inhibitor, for the treatment of advanced (unresectable or metastatic) melanoma in adults, regardless of BRAF status. The drug was approved by FDA for the treatment of patients both with BRAF V600 wild-type unresectable and BRAF V600 mutation-positive metastatic melanoma in addition to combination treatment with ipilimumab (anti-CTLA-4 antibody). With several options requiring individualized treatment, there is a great demand for validated biomarkers that can support both the primary diagnosis and preferably predict the progression of disease and response to treatment of metastatic disease. Predictive biomarkers of response to immune checkpoint inhibitors are currently under evaluation including but not limited to the lymphocytic infiltration of the tumor (= the immunoscore) [29], PD-L1 expression and or CTLA-4 expression [30].

Building upon our previous proteomics work [31] and related genomics studies [32–34], proteomics data for samples from 10 patients with lymph node metastatic melanoma (PRIDE dataset identifier: PXD001725) were referred to histopathological and clinical work-up and evaluation.

Thus, in this feasibility study, in addition to the deep mining proteomic analysis utilizing high-resolution reversed phase nano-separation in combination with mass spectrometry, we also performed in depth pathological characterization (including tissue composition, tumor characteristics and lymphocytic infiltration). The pathological analyses were performed on tumor tissues sections adjacent to the areas used for deep mining. Clinical follow-up information of the patients was reviewed and the cases were grouped into prognostic sets. Hence, the protein expression could be related to the specific cellular composition of the sample. Based on identified protein signatures, molecular classification and clinicopathological characterization, emerging biological relevance could be assigned to several marker proteins.

Materials and methods

Clinical samples

The location of primary tumors and progression of melanomas is displayed in Fig 1. This study was approved by the Regional Ethical Committee at Lund University, Southern Sweden, approval number: DNR 191/2007 and 101/2013. All patients within the study provided a written informed consent. The tumor tissues used were lymph node metastases from 10 melanoma patients undergoing surgery at Lund University Hospital, Sweden. The clinical information on respective patients is summarized in Table 1. The fresh specimens were divided into two parts. One portion of the metastasis was fixed in formalin, embedded in paraffin (FFPE) and subsequently sectioned for histopathologic confirmation and the other part was snap frozen within minutes after removal and stored at -80°C in the Biobank. All FFPE samples were routinely confirmed for diagnosis at the department of surgical pathology. The frozen specimens were used as described below for both protein expression analysis and further histological evaluations.

Histological evaluation of tumors

Frozen tissue samples were sectioned on a cryostat into 6 μm thick sections, placed upon glass slides, dried at 37°C for 30 min and fixed with 100% methanol for 5 min. The sections were stained with hematoxylin and eosin (HE) [35]. Histological examination was performed on sections immediately neighboring on both sides those sections that were solubilized and subjected to LC-MS/MS investigation. The tumor samples were analyzed for their contents regarding ratio of neoplastic area, adjacent lymph node area, necrosis and connective tissue including fat, fibrous tissue or other material. The tumor parameters were grouped and scored as referenced [21]: tumor cell size was initially measured and assigned as < 20 μm, 20–25 μm, > 25 μm; tumor cell shape was classified as epithelioid, spindle or mixed; pigmentation was scored as 0–3 (0 = no melanin pigment, 1 = slight melanin pigmentation visible at high power, 2 = moderate pigmentation visible at low power, 3 = high pigmentation readily visible at low

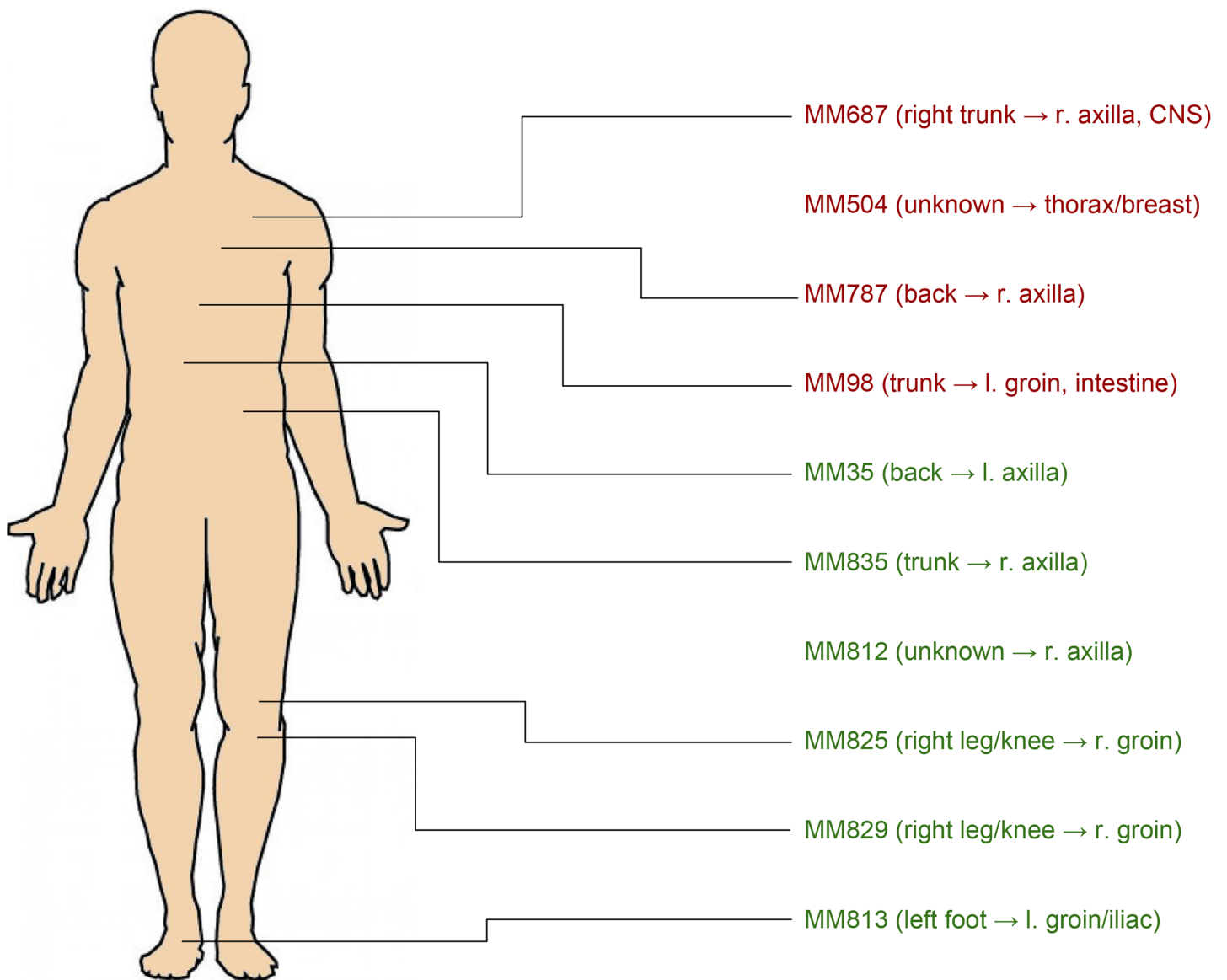


Fig 1. Location of primary tumors on the body of melanoma patients and their route of progression. Red font represents poor prognosis (“non-survivors”), green font represents good prognosis (“survivors”).

<https://doi.org/10.1371/journal.pone.0176167.g001>

Table 1. Clinical information of patient characteristics. Breslow thickness and Clarks refer to primary melanoma feature.

Tumor	Gender	Age at met	Age at primary	Breslow class	Clark	Stage	Status	OS	DSS
MM35	Male	55	54	3	4	3	Alive	7960	-
MM98	Male	75	73	4	4	3	Dead	519	519
MM504	Male	54	NA	NA	NA	NA	Dead	451	451
MM687	Male	74	72	1	2	3	Dead	591	591
MM787	Male	81	78	2	4	3	Dead	734	734
MM812	Male	51	NA	NA	NA	NA	Alive	5028	-
MM813	Female	54	54	2	3	3	Alive	4913	-
MM825	Female	66	64	2	4	3	Alive	4508	-
MM829	Male	55	49	1	2	3	Alive	4431	-
MM835	Female	36	32	3	3	3	Alive	4353	-

NA—not available

OS—Calculated from date of sample collection to 20160622.

DSS—Calculated from date of sample collection to date of dead in melanoma disease.

<https://doi.org/10.1371/journal.pone.0176167.t001>

power with dense melanin content); predominant cytoplasmic properties were assigned as unremarkable, eosinophilic or mixed. The lymphocytic infiltration in two dimensions (distribution: 0: no infiltration, 1: less than 25% of tumor infiltrated, 2: 25–50% of tumor infiltrated, 3: more than 50% of tumor infiltrated by lymphocytes; density was assessed on a 0–3 semi-quantitative scale) was assessed resulting in a combined (lymphocyte distribution + lymphocyte density) = immunoscore (sum of components: 0, 2–6).

Prognostic grouping of patients based on clinical follow-up data

For prediction of occurrence of distant organ metastases and eventually, survival we have reviewed the clinical history and the follow-up information on all 10 patients. Overall survival (OS) and disease-specific survival (DSS) of the patients were available. Kaplan-Meier survival curve supported by log-rank test was constructed (Fig 2A). In order to relate protein expression data to clinical outcome, we have identified a group of “survivors” (group 1 in Fig 2A, 2B and 2C), who did not develop any further recurrence of the neoplastic disease on a long-term follow-up period (range = 4353–7960 days) as compared to “non-survivors” (group 2 in Fig 2A, 2B and 2C) who have progressed to stage IV cancer and eventually succumbed to widespread malignant melanoma (range = 451–591 days). We excluded those cases, which had tumor tissue of less than 10% on the slides (Fig 2C), and one case which deceased without evidence of malignancy (Fig 2C). The characteristics of the tumors of the clinically and pathologically stratified patients are displayed in Table 2.

Proteomics data

Proteomics data were used, as deposited in the PRIDE database, under the dataset identifier PXD001725 [31]. At least two unique peptides were necessary for protein identification, and at the parameter Peptide Confidence in Proteome Discoverer was required to be “high”.

Bioinformatics

Initial functional analysis of protein lists used the DAVID and ConsensusPathDb tool sets [36, 37]. Enrichment of the lists in particular functional annotations was assessed by Fisher’s exact test with Benjamini correction for multiple tests. Gene Ontology annotations, SwissProt

keywords, and KEGG pathways were used as annotation terms for the enrichment analysis. For lists of proteins with significantly changed expression, the background protein sets consisted of all proteins detected. Other visualizations, list manipulations and charts were conducted in Spotfire (Tibco Software, Inc., Palo Alto, CA, USA).

Investigation of correlations between protein expression data and histopathology was performed for histological parameters: 1) tumor percentage, 2) connective tissue percentage, 3) adjacent lymph node area and 4) immunoscore. Herein, for protein expression, detection count was used as proxy for abundance. With triplicate proteomics analysis of every patient sample, detection count ranged from zero to three. Spearman rank correlation was used, in home-made scripts within the R environment.

For statistical analysis of significant differences in protein occurrences between the clinical “survivors” and “non-survivors” patient sample sets, t-test was applied as implemented in the Perseus toolkit (<http://www.coxdocs.org/doku.php?id=perseus:start>). For the purpose of this test, for each protein total PSM count was used as proxy for protein abundance, thus the t-test compared 9 vs. 9 samples for every protein (3 patients per group times 3 replicates).

For in-depth functional analysis of the set of differentially regulated proteins (“survivors” vs. “non-survivors”) and of the set of proteins correlated significantly with sample tumor content, QIAGEN’s Ingenuity Pathway Analysis (Qiagen, Redwood City, CA, USA) was used to generate relationship networks, and perform additional functional analyses.

Results and discussion

Histological characterization

The pathological evaluation is based on general directives of pathological assessment of tumor landmarks which is comparable to other studies previously performed [21], in addition to the

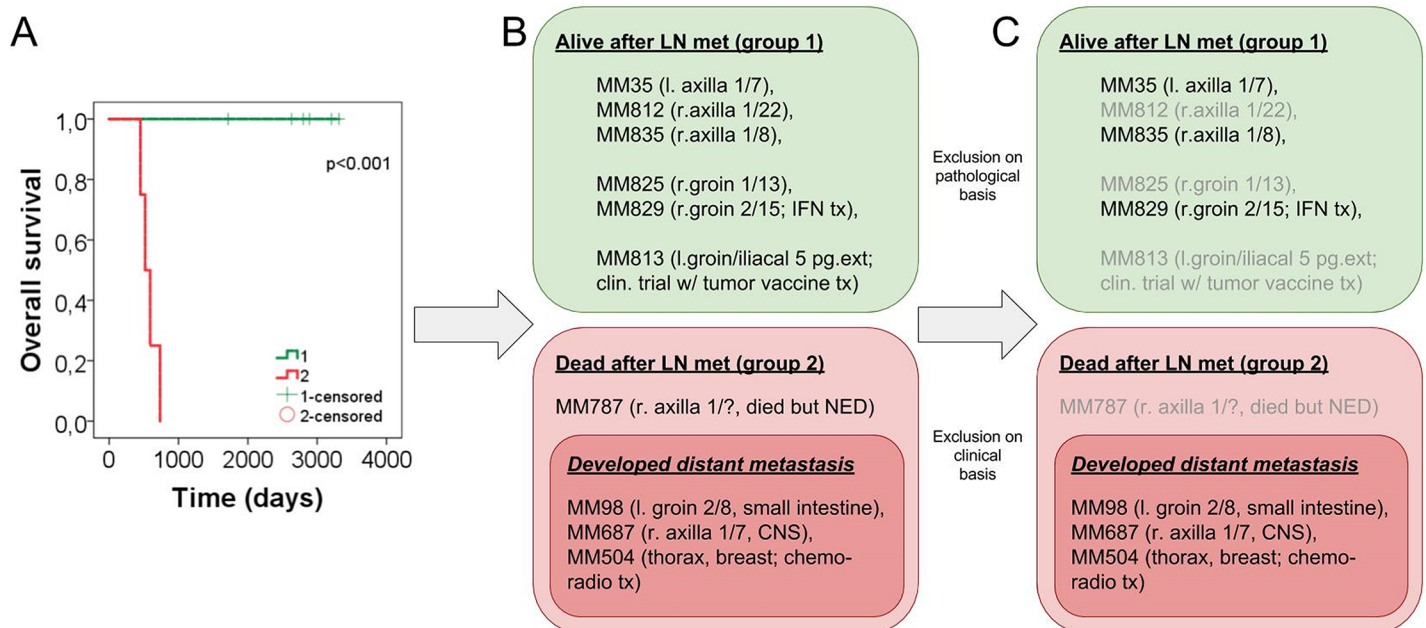


Fig 2. (A) Overall survival of the prognostic groups, “survivors” (group 1) and “non-survivors” (group 2). (B) All ten cases were subjected to rigorous review both on histological and clinical grounds. (C) Those were omitted (lighter grey text), where the tumor content of the examined tissue was low (<10%) or the clinical follow-up data resulted in non-disease-specific outcome measures (one patient in group 2 died without evidence of malignancy). Abbreviations: l: left; r: right; LN met: lymph node metastasis; CNS: central nervous system; tx: therapy. Numbers in brackets mean lymph nodes containing metastatic melanomas / all lymph nodes dissected from either the groin or the axilla: $n_{metastatic}/n_{all}$.

<https://doi.org/10.1371/journal.pone.0176167.g002>

Table 2. Histopathological properties of the melanoma metastases evaluated in this study. The ten tumors are grouped according to clinicopathological classification.

GROUPING		Clinicopathologic			
		All	Equivocal*	"survivors"	"non-survivors"
Tumor cell size	<20 microns	10	4	3	3
	20–25 microns	0	0	0	0
	>25 microns	0	0	0	0
Tumor cell shape	epithelioid	7	2	2	2
	Spindle	0	0	0	0
	Mixed	3	1	1	1
Pigment score	0	2	1	1	0
	1	2	0	0	1
	2	2	1	1	0
	3	4	1	1	2
Cytoplasm	eosinophilic	10	4	3	3
	Unremarkable	0	0	0	0
	Mixed	0	0	0	0
Lymphocyte distribution	0	0	0	0	0
	1	4	1	1	2
	2	3	2	1	1
	3	1	0	1	0
Lymphocyte density	0	0	0	0	0
	1	6	2	1	2
	2	2	1	1	1
	3	0	0	0	0
Immunoscore (= lymphocyte density+ lymphocyte distribution)	0	0	0	0	0
	2	3	1	1	1
	3	4	0	1	1
	4	0	1	0	0
	5	1	0	1	0
	6	0	0	0	0
Tumor (%)	Avg	59.4	21.3	74.6	94.6
Adjacent lymph node area (%)	Avg	27.0	50.5	21.8	0.5
Necrosis (%)	Avg	0	0	0	0
Connective tissue content (%)	avg	13.7	27.8	3.5	4.8

* equivocal cases represent those cases, which had tumor tissue of less than 10% on the slides, and one patient who deceased without evidence of malignancy.

<https://doi.org/10.1371/journal.pone.0176167.t002>

detailed pathophysiological disease status that each patient’s tissue represents. The first section of tumor tissue was stained with HE, the adjacent sections were subjected to proteomic analysis, and finally the last section was stained with HE and was also characterized by histology. The general tumor cell content of lymph nodes containing metastasis tissues was assessed, and percentages of identified areas were recorded. The melanoma metastases were also characterized for their cytological appearance: tumor cell size and shape, predominant cytoplasmic appearance in line with pigmentation. A pigment score and lymphocyte distribution and density were assessed resulting in a combined immunoscore as described in Materials and Methods (Table 2).

Our previous genomics study using the same patient samples [32], identified “high immune” and the “pigmentation” subtypes of melanoma metastases. Here, we assessed the tumors independently of their intrinsic genomic subtype. All melanoma metastases were

composed of generally small sized tumor cells (< 20 microns) with a predominantly eosinophilic cytoplasm (100%, for both properties). The shape of tumor cells was mostly epithelioid in 7 (70%) cases, while presence of admixed spindle morphology was noted in 3 (30%) cases. Melanin pigment was noted as follows; two score 0, two score 1, two score 2 and four score 3 cases were observed. Immunoscore could only be established in 8 cases, because the amount of tumor was too low ($\leq 10\%$) in two cases for accurate assessment. The lymphocyte distribution was lower than 25% of the tumor in 4 cases, was more widespread (25–50%) in 3 cases and extensive (>50%) in 1 case. The density of lymphocytes was mostly low (score 1) in 6 cases and moderate (score 2) in 2 cases. The combined immunoscore was 2, 3 and 5 in three, four and one case, respectively (Table 2).

Correlation of protein expression to histological evaluation

In this study, applying conservative criteria, more than 3000 proteins were detected in metastatic melanoma samples [31]. Investigation of correlations between protein expression data and histopathology was performed for histological parameters: 1) tumor percentage, 2) “background” connective tissue percentage, 3) adjacent lymph node area and 4) tumor immunoscore. Herein, for protein expression, detection count was used as proxy for abundance. With triplicate proteomics analysis of every patient sample, the detection count ranged from zero to three. A downside to this approach was the fact that correlation could not be calculated for 159 proteins detected in each sample.

The correlation of protein expression to tumor percentage and to immunoscore were themselves significantly correlated ($r = 0.57$, p -value $< 10^{-5}$). Among the 288 proteins significantly positively correlated to tumor percentage (shown in S1 Table), there were four proteins clearly labelled as melanoma markers: melanoma cell adhesion molecule (MUC18) [38], melanoma chondroitin sulfate proteoglycan (CSPG4) [39], melanocyte protein (PMEL, melan A), melanoma-associated antigen D2 (MAGD2). Among melanoma markers and proteins linked to this disease, alpha-synuclein and PMEL were significantly correlated to tumor percentage while S100A1 had correlation close to significance at $r = 0.61$ ($p = 0.06$). However, S100B had a low correlation to tumor percentage at $r = 0.32$ ($p = 0.37$). As many as 71 proteins were negatively correlated to tumor content, however, these may be specific to non-tumor cell types (connective tissues and/or adjacent lymph node) rather than being specific to lack of tumor shown in S2 Table.

An analysis of functional annotations over-represented among proteins correlated to tumor percentage was performed using the ConsensusPathDB and DAVID systems. Both analyses brought similar conclusions. Aminoacyl-tRNA- biosynthesis tRNA-charging was one of top pathways and biological processes significantly related to the protein set. This outcome was due to the fact that nine aminoacyl-tRNA-synthetases were significantly correlated to tumor percentage. These were those for Gln, Thr, Val, Cys, Asp, Ala, His, Arg and Ile, with the r correlation coefficient ranging from 0.67 to 0.81. Aminoacyl tRNA synthetases are believed to be involved in tumorigenesis presumably involving their additional domains which are not directly responsible to their biosynthetic activities [40]. Recently, one aminoacyl tRNA synthetase was used as a cancer drug target [41]. Other pathways and processes manifested by the proteins correlated to tumor percentage, include mitochondrial proteins (more than 80 among significantly correlated) and N-cadherin signaling (including catenins alpha-1, beta-1 and delta-1).

The set of proteins significantly correlated to tumor percentage was also subjected to Ingenuity Pathway Analysis (IPA) system. Among the “Canonical Pathways” significantly enriched in the protein set, tRNA-charging ($p = 2.7E-08$, 11 proteins out of 82) and Protein

Ubiquitination Pathway ($p = 4.7E-08$, the set included 18 proteins out of 259 pathway proteins) were most significantly related to the protein set. Other canonical pathways included Clathrin-mediated Endocytosis Signaling, Remodeling of Epithelial Adherens Junctions, Acute Phase Response Signaling, Fatty Acid β -oxidation I, EIF2 Signaling. Most of these pathways were implicated in melanoma [42–44]. Ingenuity Pathway Analysis system also yields deduced upstream regulators of a gene set. In the case of proteins correlated to tumor content, the top upstream regulators were MYC, HNF4A and TGFB1, each regulating more than 50 proteins from the query set. For MYC and TGFB1, their roles in melanoma are well-established [45, 46]. Among the general functional annotations over-represented in the query protein set, Cell Death and Survival, Cellular Growth and Proliferation, and Cellular Movement were most significant.

Another application of IPA was “Core Analysis” that considers the overall network of relationships between all human proteins and extracts sub-networks enriched in query proteins. Here, for the set of proteins correlated to tumor content, three top sub-networks, were enriched in molecules involved in Molecular Transport, Protein Trafficking, Cell Signaling (1st subnetwork, [S1A Fig](#)), DNA Replication, Recombination, and Repair, Cellular Assembly and Organization, Cell-To-Cell Signaling and Interaction (2nd subnetwork, [S1B Fig](#)) and Cancer, Organismal Injury and Abnormalities (3rd subnetwork, [S1C Fig](#)).

Correlation of protein expression to disease outcome

In order to relate, in a currently performed pilot analysis, protein expression in metastatic lymph nodes to patient survival, a t-test was performed, by comparing for every protein, the sum of PSM counts (as proxy for protein abundance) between three survivors and three non-survivors. The results (see [Fig 3A](#) and [S3 Table](#)) showed a number of significant differences, suggesting that even for these very low patient numbers, some trends can be observed. As many as 36 proteins had the t-test p-value below 0.001, and 74 proteins had p-value below 0.01 ([Fig 3B](#)). Majority of significant proteins had higher expression in non-survivors. The only well-established melanoma marker in that group was PMEL (almost 8-fold more abundant in patients who progressed). However, many proteins from this list have previously been linked to melanoma in the literature ([Fig 3C](#)).

Strikingly, most significant in relation to patient survival is HEXB, or Beta-hexosaminidase subunit beta. This lysosomal enzyme is involved in hydrolysis of gangliosides GM2 to GM3. A recent study by Tringali et al showed that poor survival in melanoma is significantly related to GM3 levels [47]. These data agree well with our preliminary finding of elevated HEXB levels in patients with poor survival. Another study reported that increased levels of a related ganglioside GD3 increase malignant properties of melanoma cells [48], thus supporting the hypothesis that imbalance in ganglioside forms may contribute to melanoma severity and poor survival. The HEXB protein was also noted by Byrum et al as differing between primary melanoma, benign nevi and MM, but the direction of changes they reported was different [49].

Other proteins most significantly differing between survivors and non-survivors were GPNMB (glycoprotein non-metastatic melanoma protein B, a homologue of PMEL) and PKM (pyruvate kinase, muscle) hemopexin (HPX), complement factors (C3, C4B and CFH) and vinculin (VCL), Annexin A5 (ANXA5), V-type proton ATPase catalytic subunits (ATP6V1A, ATP6V1B2) and two aminoacyl tRNA ligases (VARS and IARS2). GPNMB was shown previously to be linked to metastasis, and is in clinical trials for melanoma [50]. PKM controls glycolysis, a process crucial for metabolism in malignant cells, and the balance of splicing-derived PKM isoforms is known to be related to cancer invasiveness [51, 52]. The Complement C3a Receptor signaling has been very recently shown to contribute to melanoma tumorigenesis

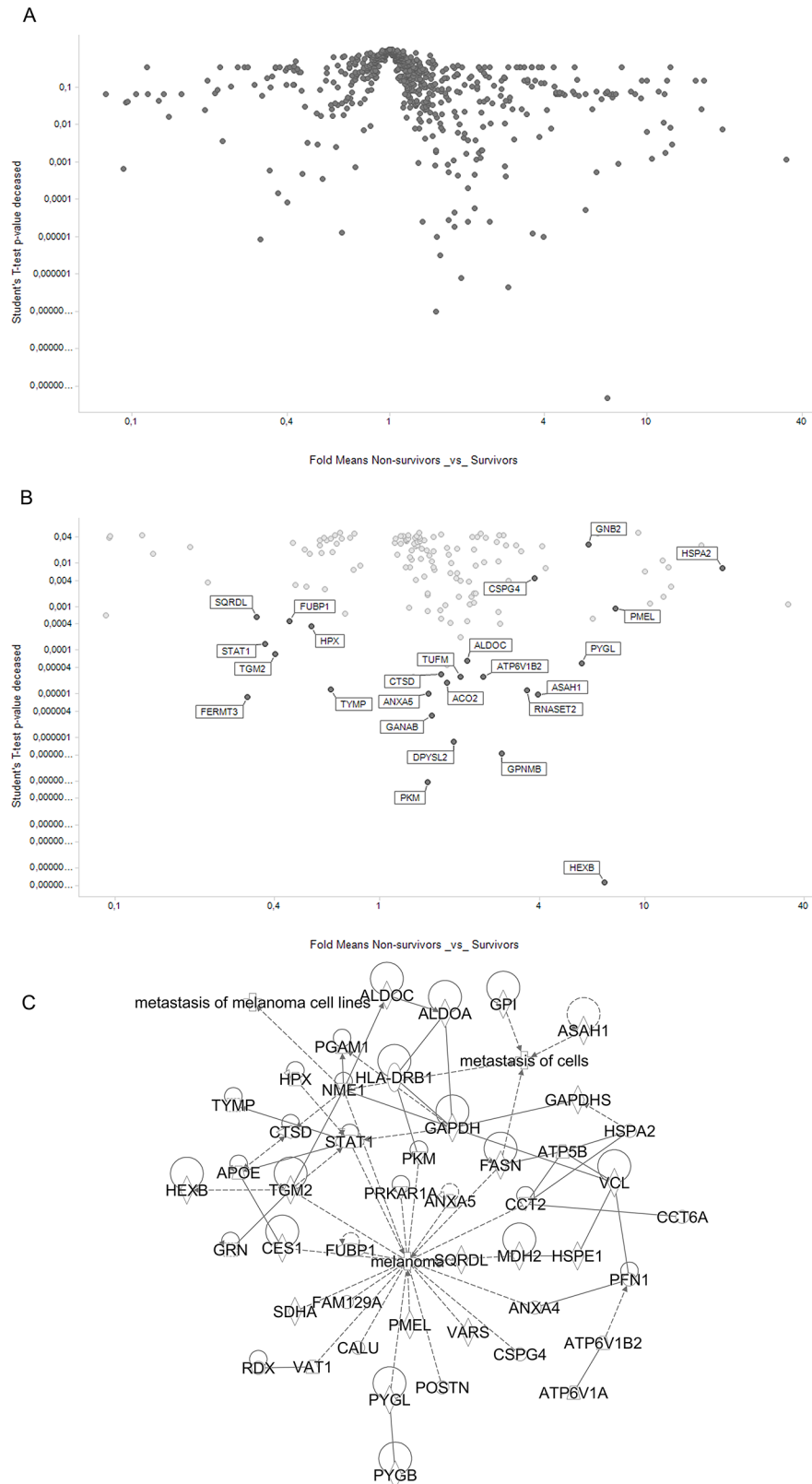


Fig 3. (A) Volcano plot showing differences in approximate protein abundance between survivors and non-survivors. T-test p-value and mean fold difference shown (protein abundance evaluated as sum of PSMs). **(B)**

As in (A), but only significant proteins shown ($p < 0.05$). (C) Biological relationship network (IPA) for proteins differentiating between survivors and non-survivors (shown in B), and having literature links to melanoma or metastasis. Only significant proteins shown (T-test p -value below 0.01), excluding proteins having no IPA relationships within the presented set.

<https://doi.org/10.1371/journal.pone.0176167.g003>

[53]. On the contrary, differential expression of vinculin between weakly and highly metastatic melanoma cell lines was noted more than 20 years ago [54].

The IPA analysis was performed for the sets of proteins that differed between survivors and non-survivors (S2 Fig and S3A–S3D Fig). Core IPA analysis revealed that most significant canonical pathway enriched in the set of proteins changed between survivors and non-survivors was glycolysis (p -value $9.8E-13$) while cell death and survival, carbohydrate metabolism, cellular movement, and cellular growth and proliferation were the most significant biological functions overrepresented in this protein set. This is consistent with biological processes known to be related to metastatic properties of cancer.

Despite a very small number of patients in this pilot evaluation, (three survivors and three non-survivors), a number of proteins were found to differentiate the two groups, and substantial number of these was previously linked to cancer in the literature (S2 Fig). Among the proteins most significantly differentiating between the two patient groups, HEXB, PKM and GPNMB stood out, as hallmarks of processes involved in melanoma progression and responsible for poor survival.

Conclusion

An in depth pathological analysis of metastatic melanoma samples used for generating deep mining high-quality mass spectrometry data of protein expression is presented. This feasibility study provides an example how clinical outcome and detailed histopathology analysis related to proteomics discovery data can provide novel insights into the molecular processes driving the disease. The main implication of this study is that melanoma proteomics should be inseparable from histological evaluation performed in the most detailed manner. This unique approach is the main strength of this study while it has obvious limitations arising from

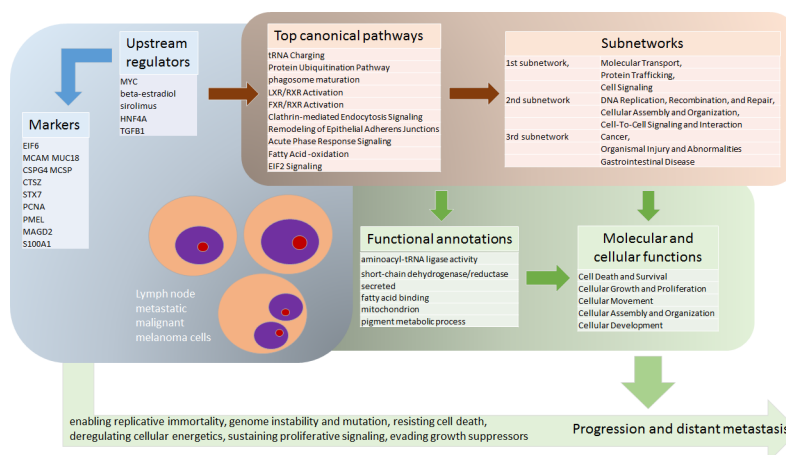


Fig 4. Identified melanoma markers and pathobiological processes in tissue samples of melanoma lymph node metastases. The graphics displays key upstream regulators found according to analysis based on DAVID and IPA evaluation. The graph displays major regulated canonical pathways and subnetworks resulting in cellular functions and molecular fingerprints providing survival advantage for malignant cells with promotion to further progression and metastasis.

<https://doi.org/10.1371/journal.pone.0176167.g004>

relatively limited number of patient samples. The mass spectrometry data represent the initial stage of a protein sequence database for metastatic melanoma. The combined knowledge of the tumor cellular composition with protein expression of each metastasis enables identification of novel, significantly regulated proteins, in melanoma tumor tissue sections. Upon further validation and development these proteins might serve as future diagnostic markers for this cancer. In Fig 4, the key upstream regulators, the major regulated canonical pathways and subnetworks according to analysis based on DAVID and IPA evaluation are summarized. Cellular functions and molecular fingerprints that provide survival advantage for malignant cells with promotion to further disease progression were highly represented in our overall analysis. In addition, several markers previously related to melanoma were seen to correlate to the tissue tumor cell content. Although the translational impact of this feasibility study is not immediate, future studies should confirm the relevance of such proteins as important melanoma landmarks.

Supporting information

S1 Fig. (A) First, (B) second and (C) third most significant biological relationship subnetworks resulting from Ingenuity Pathways Analysis (IPA) for the proteins correlated to tumor content. Members of the original list of 359 proteins marked in grey. Magenta outline highlights proteins implicated in cancer according to IPA database.
(TIF)

S2 Fig. Subcellular locations and biological relationship network for proteins differentiating between survivors and non-survivors. Only significant proteins were shown (t-test, p-value below 0.01). Known cancer biomarkers marked by magenta outline (IPA). Proteins having no IPA relationships within the presented set are excluded. Red filling: proteins with higher expression in non-survivors.
(TIF)

S3 Fig. (A) First, (B) second, (C) third and (D) fourth, respectively, most significant biological relationship subnetworks resulting from Ingenuity Pathways Analysis for the proteins differentiating between survivors and non-survivors. Only significant proteins used in the IPA analysis (T-test p-value below 0.01). Known cancer biomarkers marked by magenta outline. Red filling: proteins with higher expression in non-survivors.
(TIF)

S1 Table. Proteins significantly positively correlated to tumor content.
(XLSX)

S2 Table. Proteins significantly negatively correlated to tumor content.
(XLSX)

S3 Table. Correlation of protein expression to disease outcome. Student's t-test p-value provided for comparison of survivors vs non-survivors. PSM counts compared, three patients in a group, each in triplicate, hence 9 samples per group.
(XLSX)

Acknowledgments

We thank Dr. Dariusz Gozdowski for helpful discussions and advice in statistical issues.

This study is dedicated to the memory of Dr. Thomas Edward Fehniger, our colleague and dear friend who left us far too early.

Author Contributions

Conceptualization: CW KP AMS EW GMV.

Formal analysis: KP AMS.

Funding acquisition: CW GMV.

Investigation: CW KP AMS EW GMV MR MY YS.

Methodology: CW KP AMS EW GMV MR MY YS.

Project administration: CW KP AMS EW GMV.

Resources: CW KP AMS EW GMV GJ CI LL BB HO.

Supervision: CW KP AMS EW GMV.

Validation: CW KP AMS EW GMV MR.

Visualization: CW KP AMS EW GMV.

Writing – original draft: CW KP AMS EW GMV.

Writing – review & editing: CW KP AMS EW GMV MR MY YS JM GJ CI LL BB HO TL.

References

- Merrill RM, Bateman S. Conditional Melanoma Cancer Survival in the United States. *Cancers*. 2016; 8 (2). Epub 2016/02/06. PubMed Central PMCID: PMC4773743.
- Thiam A, Zhao Z, Quinn C, Barber B. Years of life lost due to metastatic melanoma in 12 countries. *Journal of medical economics*. 2016; 19(3):259–64. Epub 2015/11/05. <https://doi.org/10.3111/13696998.2015.1115764> PMID: 26531249
- Berwick M, Buller DB, Cust A, Gallagher R, Lee TK, Meyskens F, et al. Melanoma Epidemiology and Prevention. *Cancer treatment and research*. 2016; 167:17–49. Epub 2015/11/26. https://doi.org/10.1007/978-3-319-22539-5_2 PMID: 26601858
- Eriksson H, Lyth J, Andersson TM. The proportion cured of patients diagnosed with Stage III-IV cutaneous malignant melanoma in Sweden 1990–2007: A population-based study. *International journal of cancer Journal international du cancer*. 2016; 138(12):2829–36. Epub 2016/01/28. <https://doi.org/10.1002/ijc.30023> PMID: 26815934
- Hanahan D, Weinberg RA. The hallmarks of cancer. *Cell*. 2000; 100(1):57–70. Epub 2000/01/27. PMID: 10647931
- Hanahan D, Weinberg RA. Hallmarks of cancer: the next generation. *Cell*. 2011; 144(5):646–74. Epub 2011/03/08. <https://doi.org/10.1016/j.cell.2011.02.013> PMID: 21376230
- Valsecchi ME, Silbermins D, de Rosa N, Wong SL, Lyman GH. Lymphatic mapping and sentinel lymph node biopsy in patients with melanoma: a meta-analysis. *Journal of clinical oncology: official journal of the American Society of Clinical Oncology*. 2011; 29(11):1479–87. Epub 2011/03/09.
- Tas F. Metastatic behavior in melanoma: timing, pattern, survival, and influencing factors. *Journal of oncology*. 2012; 2012:647684. Epub 2012/07/14. PubMed Central PMCID: PMC3391929. <https://doi.org/10.1155/2012/647684> PMID: 22792102
- Morton DL. Overview and update of the phase III Multicenter Selective Lymphadenectomy Trials (MSLT-I and MSLT-II) in melanoma. *Clinical & experimental metastasis*. 2012; 29(7):699–706. Epub 2012/06/26. PubMed Central PMCID: PMC3463679.
- Breslow A. Thickness, cross-sectional areas and depth of invasion in the prognosis of cutaneous melanoma. *Annals of surgery*. 1970; 172(5):902–8. Epub 1970/11/01. PubMed Central PMCID: PMC1397358. PMID: 5477666
- Balch CM, Murad TM, Soong SJ, Ingalls AL, Halpern NB, Maddox WA. A multifactorial analysis of melanoma: prognostic histopathological features comparing Clark's and Breslow's staging methods. *Annals of surgery*. 1978; 188(6):732–42. Epub 1978/12/01. PubMed Central PMCID: PMC1397001. PMID: 736651

12. Eldh J, Boeryd B, Peterson LE. Prognostic factors in cutaneous malignant melanoma in stage I. A clinical, morphological and multivariate analysis. *Scandinavian journal of plastic and reconstructive surgery*. 1978; 12(3):243–55. Epub 1978/01/01. PMID: [741213](#)
13. Van Der Esch EP, Cascinelli N, Preda F, Morabito A, Bufalino R. Stage I melanoma of the skin: evaluation of prognosis according to histologic characteristics. *Cancer*. 1981; 48(7):1668–73. Epub 1981/10/01. PMID: [7284966](#)
14. Jakob JA, Bassett RL Jr., Ng CS, Curry JL, Joseph RW, Alvarado GC, et al. NRAS mutation status is an independent prognostic factor in metastatic melanoma. *Cancer*. 2012; 118(16):4014–23. Epub 2011/12/20. PubMed Central PMCID: PMCPmc3310961. <https://doi.org/10.1002/cncr.26724> PMID: [22180178](#)
15. Kim DW, Haydu LE, Joon AY, Bassett RL Jr., Siroy AE, Tetzlaff MT, et al. Clinicopathological features and clinical outcomes associated with TP53 and BRAFNon-V600 mutations in cutaneous melanoma patients. *Cancer*. 2016. Epub 2016/12/03.
16. Schlaak M, Bajah A, Podewski T, Kreuzberg N, von Bartenwerffer W, Wardelmann E, et al. Assessment of clinical parameters associated with mutational status in metastatic malignant melanoma: a single-centre investigation of 141 patients. *The British journal of dermatology*. 2013; 168(4):708–16. Epub 2013/03/27. <https://doi.org/10.1111/bjd.12140> PMID: [23528057](#)
17. Meckbach D, Bauer J, Pflugfelder A, Meier F, Busch C, Eigentler TK, et al. Survival according to BRAF-V600 tumor mutations—an analysis of 437 patients with primary melanoma. *PloS one*. 2014; 9(1):e86194. Epub 2014/01/30. PubMed Central PMCID: PMCPmc3901680. <https://doi.org/10.1371/journal.pone.0086194> PMID: [24475086](#)
18. Huang FW, Hodis E, Xu MJ, Kryukov GV, Chin L, Garraway LA. Highly recurrent TERT promoter mutations in human melanoma. *Science (New York, NY)*. 2013; 339(6122):957–9. Epub 2013/01/26. PubMed Central PMCID: PMCPmc4423787.
19. Killela PJ, Reitman ZJ, Jiao Y, Bettgowda C, Agrawal N, Diaz LA Jr., et al. TERT promoter mutations occur frequently in gliomas and a subset of tumors derived from cells with low rates of self-renewal. *Proceedings of the National Academy of Sciences of the United States of America*. 2013; 110(15):6021–6. Epub 2013/03/27. PubMed Central PMCID: PMCPmc3625331. <https://doi.org/10.1073/pnas.1303607110> PMID: [23530248](#)
20. Bucheit AD, Syklawer E, Jakob JA, Bassett RL Jr., Curry JL, Gershenwald JE, et al. Clinical characteristics and outcomes with specific BRAF and NRAS mutations in patients with metastatic melanoma. *Cancer*. 2013; 119(21):3821–9. Epub 2013/08/08. <https://doi.org/10.1002/cncr.28306> PMID: [23922205](#)
21. Network TCGAR. Genomic Classification of Cutaneous Melanoma. *Cell*. 2015; 161:1681–96. <https://doi.org/10.1016/j.cell.2015.05.044> PMID: [26091043](#)
22. Ascierto PA, Kirkwood JM, Grob JJ, Simeone E, Grimaldi AM, Maio M, et al. The role of BRAF V600 mutation in melanoma. *Journal of translational medicine*. 2012; 10:85. Epub 2012/05/05. PubMed Central PMCID: PMCPmc3391993. <https://doi.org/10.1186/1479-5876-10-85> PMID: [22554099](#)
23. Bollag G, Hirth P, Tsai J, Zhang J, Ibrahim PN, Cho H, et al. Clinical efficacy of a RAF inhibitor needs broad target blockade in BRAF-mutant melanoma. *Nature*. 2010; 467(7315):596–9. Epub 2010/09/09. PubMed Central PMCID: PMCPmc2948082. <https://doi.org/10.1038/nature09454> PMID: [20823850](#)
24. Chapman PB, Hauschild A, Robert C, Haanen JB, Ascierto P, Larkin J, et al. Improved survival with vemurafenib in melanoma with BRAF V600E mutation. *The New England journal of medicine*. 2011; 364(26):2507–16. Epub 2011/06/07. PubMed Central PMCID: PMCPmc3549296. <https://doi.org/10.1056/NEJMoa1103782> PMID: [21639808](#)
25. Hodi FS, O'Day SJ, McDermott DF, Weber RW, Sosman JA, Haanen JB, et al. Improved survival with ipilimumab in patients with metastatic melanoma. *The New England journal of medicine*. 2010; 363(8):711–23. Epub 2010/06/08. PubMed Central PMCID: PMCPmc3549297. <https://doi.org/10.1056/NEJMoa1003466> PMID: [20525992](#)
26. Rizos H, Menzies AM, Pupo GM, Carlino MS, Fung C, Hyman J, et al. BRAF inhibitor resistance mechanisms in metastatic melanoma: spectrum and clinical impact. *Clinical cancer research: an official journal of the American Association for Cancer Research*. 2014; 20(7):1965–77. Epub 2014/01/28.
27. Sugihara Y, Vegvari A, Welinder C, Jonsson G, Ingvar C, Lundgren L, et al. A new look at drugs targeting malignant melanoma—an application for mass spectrometry imaging. *Proteomics*. 2014; 14(17–18):1963–70. Epub 2014/07/22. <https://doi.org/10.1002/pmhc.201300476> PMID: [25044963](#)
28. Sun C, Wang L, Huang S, Heynen GJ, Prahallad A, Robert C, et al. Reversible and adaptive resistance to BRAF(V600E) inhibition in melanoma. *Nature*. 2014; 508(7494):118–22. Epub 2014/03/29. <https://doi.org/10.1038/nature13121> PMID: [24670642](#)
29. Galon J, Pages F, Marincola FM, Angell HK, Thurin M, Lugli A, et al. Cancer classification using the Immunoscore: a worldwide task force. *Journal of translational medicine*. 2012; 10:205. Epub 2012/10/

05. PubMed Central PMCID: PMCPMC3554496. <https://doi.org/10.1186/1479-5876-10-205> PMID: 23034130
30. Pardoll DM. The blockade of immune checkpoints in cancer immunotherapy. *Nature reviews Cancer*. 2012; 12(4):252–64. Epub 2012/03/23. PubMed Central PMCID: PMCPMC4856023. <https://doi.org/10.1038/nrc3239> PMID: 22437870
31. Welinder C, Pawlowski K, Sugihara Y, Yakovleva M, Jonsson G, Ingvar C, et al. A protein deep sequencing evaluation of metastatic melanoma tissues. *PloS one*. 2015; 10(4):e0123661. Epub 2015/04/16. PubMed Central PMCID: PMCPMC4395420. <https://doi.org/10.1371/journal.pone.0123661> PMID: 25874936
32. Cirenajwis H, Ekedahl H, Lauss M, Harbst K, Carneiro A, Enoksson J, et al. Molecular stratification of metastatic melanoma using gene expression profiling: Prediction of survival outcome and benefit from molecular targeted therapy. *Oncotarget*. 2015; 6(14):12297–309. Epub 2015/04/25. PubMed Central PMCID: PMCPMC4494939. <https://doi.org/10.18632/oncotarget.3655> PMID: 25909218
33. Harbst K, Staaf J, Lauss M, Karlsson A, Masback A, Johansson I, et al. Molecular profiling reveals low- and high-grade forms of primary melanoma. *Clinical cancer research: an official journal of the American Association for Cancer Research*. 2012; 18(15):4026–36. Epub 2012/06/08. PubMed Central PMCID: PMCPMC3467105.
34. Jonsson G, Busch C, Knappskog S, Geisler J, Miletic H, Ringner M, et al. Gene expression profiling-based identification of molecular subtypes in stage IV melanomas with different clinical outcome. *Clinical cancer research: an official journal of the American Association for Cancer Research*. 2010; 16(13):3356–67. Epub 2010/05/13.
35. Lillie RD. *Histopathologic technic and practical histochemistry*. 3rd ed. New York: McGraw-Hill Book Co; 1965.
36. Huang da W, Sherman BT, Lempicki RA. Systematic and integrative analysis of large gene lists using DAVID bioinformatics resources. *Nature protocols*. 2009; 4(1):44–57. Epub 2009/01/10. <https://doi.org/10.1038/nprot.2008.211> PMID: 19131956
37. Kamburov A, Pentchev K, Galicka H, Wierling C, Lehrach H, Herwig R. ConsensusPathDB: toward a more complete picture of cell biology. *Nucleic acids research*. 2011; 39(Database issue):D712–7. Epub 2010/11/13. PubMed Central PMCID: PMCPMC3013724. <https://doi.org/10.1093/nar/gkq1156> PMID: 21071422
38. Lehmann JM, Riethmuller G, Johnson JP. MUC18, a marker of tumor progression in human melanoma, shows sequence similarity to the neural cell adhesion molecules of the immunoglobulin superfamily. *Proceedings of the National Academy of Sciences of the United States of America*. 1989; 86(24):9891–5. Epub 1989/12/01. PubMed Central PMCID: PMCPMC298608. PMID: 2602381
39. Price MA, Colvin Wanshura LE, Yang J, Carlson J, Xiang B, Li G, et al. CSPG4, a potential therapeutic target, facilitates malignant progression of melanoma. *Pigment cell & melanoma research*. 2011; 24(6):1148–57. Epub 2011/10/19. PubMed Central PMCID: PMCPMC3426219.
40. Kim S, You S, Hwang D. Aminoacyl-tRNA synthetases and tumorigenesis: more than housekeeping. *Nature reviews Cancer*. 2011; 11(10):708–18. Epub 2011/09/24. <https://doi.org/10.1038/nrc3124> PMID: 21941282
41. Gao G, Yao Y, Li K, Mashausi DS, Li D, Negi H, et al. A human leucyl-tRNA synthetase as an anticancer target. *OncoTargets and therapy*. 2015; 8:2933–42. Epub 2015/10/29. PubMed Central PMCID: PMCPMC4610879. <https://doi.org/10.2147/OTT.S88873> PMID: 26508878
42. Jayagopal A, Yang JL, Haselton FR, Chang MS. Tight junction-associated signaling pathways modulate cell proliferation in uveal melanoma. *Investigative ophthalmology & visual science*. 2011; 52(1):588–93. Epub 2010/09/24. PubMed Central PMCID: PMCPMC3053300.
43. Rodrigues MF, Obre E, de Melo FH, Santos GC Jr., Galina A, Jasiulionis MG, et al. Enhanced OXPHOS, glutaminolysis and beta-oxidation constitute the metastatic phenotype of melanoma cells. *The Biochemical journal*. 2016; 473(6):703–15. Epub 2015/12/25. <https://doi.org/10.1042/BJ20150645> PMID: 26699902
44. Wengrod J, Wang D, Weiss S, Zhong H, Osman I, Gardner LB. Phosphorylation of eIF2alpha triggered by mTORC1 inhibition and PP6C activation is required for autophagy and is aberrant in PP6C-mutated melanoma. *Science signaling*. 2015; 8(367):ra27. Epub 2015/03/12. PubMed Central PMCID: PMCPMC4580977. <https://doi.org/10.1126/scisignal.aaa0899> PMID: 25759478
45. Fico A, Alfano D, Valentino A, Vasta V, Cavalcanti E, Travali S, et al. c-Myc modulation: a key role in melanoma drug response. *Cancer biology & therapy*. 2015; 16(9):1375–86. Epub 2015/04/04. PubMed Central PMCID: PMCPMC4622542.
46. Qu X, Shen L, Zheng Y, Cui Y, Feng Z, Liu F, et al. A signal transduction pathway from TGF-beta1 to SKP2 via Akt1 and c-Myc and its correlation with progression in human melanoma. *The Journal of*

- investigative dermatology. 2014; 134(1):159–67. Epub 2013/06/25. <https://doi.org/10.1038/jid.2013.281> PMID: [23792459](https://pubmed.ncbi.nlm.nih.gov/23792459/)
47. Tringali C, Silvestri I, Testa F, Baldassari P, Anastasia L, Mortarini R, et al. Molecular subtyping of metastatic melanoma based on cell ganglioside metabolism profiles. *BMC cancer*. 2014; 14:560. Epub 2014/08/03. PubMed Central PMCID: PMCPmc4132924. <https://doi.org/10.1186/1471-2407-14-560> PMID: [25085576](https://pubmed.ncbi.nlm.nih.gov/25085576/)
 48. Ohkawa Y, Miyazaki S, Hamamura K, Kambe M, Miyata M, Tajima O, et al. Ganglioside GD3 enhances adhesion signals and augments malignant properties of melanoma cells by recruiting integrins to glycolipid-enriched microdomains. *The Journal of biological chemistry*. 2010; 285(35):27213–23. Epub 2010/06/29. PubMed Central PMCID: PMCPmc2930720. <https://doi.org/10.1074/jbc.M109.087791> PMID: [20581115](https://pubmed.ncbi.nlm.nih.gov/20581115/)
 49. Byrum SD, Larson SK, Avaritt NL, Moreland LE, Mackintosh SG, Cheung WL, et al. Quantitative Proteomics Identifies Activation of Hallmark Pathways of Cancer in Patient Melanoma. *Journal of proteomics & bioinformatics*. 2013; 6(3):43–50. Epub 2013/08/27. PubMed Central PMCID: PMCPmc3748992.
 50. Maric G, Rose AA, Annis MG, Siegel PM. Glycoprotein non-metastatic b (GPNMB): A metastatic mediator and emerging therapeutic target in cancer. *OncoTargets and therapy*. 2013; 6:839–52. Epub 2013/07/23. PubMed Central PMCID: PMCPmc3711880. <https://doi.org/10.2147/OTT.S44906> PMID: [23874106](https://pubmed.ncbi.nlm.nih.gov/23874106/)
 51. Israelsen WJ, Vander Heiden MG. Pyruvate kinase: Function, regulation and role in cancer. *Seminars in cell & developmental biology*. 2015; 43:43–51. Epub 2015/08/19. PubMed Central PMCID: PMCPmc4662905.
 52. Wang S, Yang Z, Gao Y, Li Q, Su Y, Wang Y, et al. Pyruvate kinase, muscle isoform 2 promotes proliferation and insulin secretion of pancreatic beta-cells via activating Wnt/CTNNB1 signaling. *International journal of clinical and experimental pathology*. 2015; 8(11):14441–8. Epub 2016/01/30. PubMed Central PMCID: PMCPmc4713547. PMID: [26823761](https://pubmed.ncbi.nlm.nih.gov/26823761/)
 53. Nabizadeh JA, Manthey HD, Steyn FJ, Chen W, Widiapradja A, Md Akhir FN, et al. The Complement C3a Receptor Contributes to Melanoma Tumorigenesis by Inhibiting Neutrophil and CD4+ T Cell Responses. *Journal of immunology (Baltimore, Md: 1950)*. 2016; 196(11):4783–92. Epub 2016/05/18.
 54. Sadano H, Inoue M, Taniguchi S. Differential expression of vinculin between weakly and highly metastatic B16-melanoma cell lines. *Japanese journal of cancer research: Gann*. 1992; 83(6):625–30. Epub 1992/06/01. PMID: [1644665](https://pubmed.ncbi.nlm.nih.gov/1644665/)